

University of Windsor

## Scholarship at UWindsor

---

Electronic Theses and Dissertations

Theses, Dissertations, and Major Papers

---

1-1-1967

### Radiation damage in selected crystals at low temperature.

Robert G. Wilson  
*University of Windsor*

Follow this and additional works at: <https://scholar.uwindsor.ca/etd>

---

#### Recommended Citation

Wilson, Robert G., "Radiation damage in selected crystals at low temperature." (1967). *Electronic Theses and Dissertations*. 6506.

<https://scholar.uwindsor.ca/etd/6506>

This online database contains the full-text of PhD dissertations and Masters' theses of University of Windsor students from 1954 forward. These documents are made available for personal study and research purposes only, in accordance with the Canadian Copyright Act and the Creative Commons license—CC BY-NC-ND (Attribution, Non-Commercial, No Derivative Works). Under this license, works must always be attributed to the copyright holder (original author), cannot be used for any commercial purposes, and may not be altered. Any other use would require the permission of the copyright holder. Students may inquire about withdrawing their dissertation and/or thesis from this database. For additional inquiries, please contact the repository administrator via email ([scholarship@uwindsor.ca](mailto:scholarship@uwindsor.ca)) or by telephone at 519-253-3000ext. 3208.

RADIATION DAMAGE IN SELECTED CRYSTALS  
AT LOW TEMPERATURE

by

Robert G. Wilson

A Thesis  
Submitted to the Faculty of Graduate Studies through the Department  
of Physics in Partial Fulfillment of the Requirements for  
the Degree of Master of Science at the  
University of Windsor

Windsor, Ontario

1967

UMI Number: EC52688

### INFORMATION TO USERS

The quality of this reproduction is dependent upon the quality of the copy submitted. Broken or indistinct print, colored or poor quality illustrations and photographs, print bleed-through, substandard margins, and improper alignment can adversely affect reproduction.

In the unlikely event that the author did not send a complete manuscript and there are missing pages, these will be noted. Also, if unauthorized copyright material had to be removed, a note will indicate the deletion.

**UMI**<sup>®</sup>

---

UMI Microform EC52688

Copyright 2008 by ProQuest LLC.

All rights reserved. This microform edition is protected against unauthorized copying under Title 17, United States Code.

ProQuest LLC  
789 E. Eisenhower Parkway  
PO Box 1346  
Ann Arbor, MI 48106-1346

APPROVED BY:

F. Holuj

Dr. F. Holuj (Chairman)

N. E. Hedgecock

Dr. N. E. Hedgecock

Gordon Wood

Dr. G. W. Wood

177171

### ABSTRACT

The electron paramagnetic resonance spectra of Phenacite ( $\text{Be}_2\text{SiO}_4$ ), of  $\text{CaF}_2:\text{Fe}$ , and of  $\text{BaF}_2:\text{Cr}$  samples have been studied qualitatively following x-irradiation at low temperature ( $100^\circ\text{K}$ ). In the cases of the Phenacite and the  $\text{CaF}_2:\text{Fe}$  samples, the spectra observed before irradiation differed from those obtained after irradiation. These changes indicate the presence of paramagnetic radiation damage centres in these samples following exposure to x-rays at low temperature. In the case of the  $\text{BaF}_2:\text{Cr}$  sample, however, no spectrum was observed at  $100^\circ\text{K}$ , either before or after it was x-irradiated.

#### ACKNOWLEDGEMENTS

The author wishes to thank Dr. F. Holuj for the suggestion of the problem and for guidance during the course of the research. Thanks are also extended to Mr. W. Grewe and the machine shop staff for construction of apparatus, and, in particular, for their efforts pertaining to the cryostat.

## TABLE OF CONTENTS

	Page
ABSTRACT	iii
ACKNOWLEDGEMENTS	iv
LIST OF FIGURES	vi
I. INTRODUCTION	1
A. Historical	1
B. EPR and Radiation Damage Centres	2
C. Low Temperature Radiation Damage in Crystals	3
II. INSTRUMENTATION	4
A. X-Band Bridge Spectrometer	4
B. Cryostat for Low Temperature Radiation Damage Studies	4
C. Sample Alignment	10
D. Sample and Cavity Temperatures	12
III. EXPERIMENTAL PROCEDURE	14
IV. RESULTS AND DISCUSSION	15
A. Phenacite	15
B. Calcium Fluoride Containing Iron Impurities	15
C. Barium Fluoride Containing Chromium Impurities	19
REFERENCES	24
VITA AUCTORIS	25

## LIST OF FIGURES

	Page
1. Block Diagram of X-Band Spectrometer used for EPR Experiments near 77°K	5
2. Cross Section of EPR Cryostat used to Study Low Temperature Radiation Damage in Crystals	6
3. Vacuum Seal for Crystal Rotator	8
4. Cut-Away View of the Cryostat Tail Assembly	9
5. Cross Section of Resonant Cavity Adapted for 100 kc Field Modulation	11
6. (a) Method of Sample Alignment for X-Irradiation (b) Print of Film Exposure Outlining the X-Ray Beam Arriving (i) in Front of the Cavity; (ii) at the Sample Site; (iii) at the Back Wall of the Cavity	13
7. Comparison of Phenacite Spectrum (a) at 100°K Before Irradiation, (b) at 100°K after Irradiation, and (c) at Room Temperature Following X-Irradiation at 100°K	16
8. A Detailed Comparison of the Central Group of Spectrum in Phenacite (a) at 100°K Before X-Irradiation, (b) at 100°K After X-Irradiation, and (c) at Room Temperature Following X-Irradiation at 100°K	17
9. Comparison of CaF <sub>2</sub> :Fe Spectrum (a) at 100°K Before X-Irradiation, (b) at 100°K after X-Irradiation, and (c) at Room Temperature Following X-Irradiation at 100°K	18
10. Comparison of CaF <sub>2</sub> :Fe Spectrum at a Second Orientation (a) at 100°K Before Irradiation, and (b) at 100°K After Irradiation	20
11. Changes in the CaF <sub>2</sub> :Fe Spectrum during the Warming Period Following X-Irradiation at 100°K	21
12. EPR Spectrum of BaF <sub>2</sub> :Cr (a) at 100°K Before X-Irradiation, and (b) at 100°K After Irradiation	22



## I. INTRODUCTION

### A. Historical

Irradiation of a solid by x-rays, by  $\gamma$ -rays, and by other high energy particles, usually is accompanied by radiation damage. This damage may assume the form of atomic displacements from lattice positions, of ionization of atoms and of ions, or of electronic excitations, depending on the energy of the incident radiation. For the case of x-irradiation, radiation damage is restricted either to electronic excitations, or to ionization processes.

Radiation damage in solids was first studied as early as 1896 when Goldstein<sup>1</sup> coloured ionic solids, such as the alkali halides, by high energy radiation. Review articles concerning colour centres in alkali halides have been published by Pohl<sup>2</sup>, by Seitz<sup>3</sup>, by Pick<sup>4</sup>, and by Seidel and Wolf<sup>5</sup>. Moreover, the technique of paramagnetic resonance absorption was introduced to the field as early as 1949 by Hutchinson<sup>6</sup> in his study of radiation-produced colour centres in alkali halides. Since then, electron paramagnetic resonance (EPR) has become a most useful tool with which to probe radiation damage in solids.

In the last fifteen years, the field of radiation damage has been extended to include other types of solids. Among these are the alkaline earth halides, particularly the fluorides of calcium and barium. Until now, however, radiation damage has not been studied in these crystals when they contain first series transition metal ion impurities. Samples

of  $\text{BaF}_2:\text{Cr}$  and  $\text{CaF}_2:\text{Fe}$  have been x-irradiated at a temperature near the boiling point of nitrogen and qualitatively studied using EPR methods. Natural phenacite ( $\text{Be}_2\text{SiO}_4$ ) has also been investigated.

#### B. EPR and Radiation Damage Centres

The general hamiltonian which describes the interaction energy of a paramagnetic centre located in a constant magnetic field assumes the form:

$$\begin{aligned} H &= H_{el} + H_{cf} + H_{ls} + H_{ss} + H_{zee} + H_{hfs} + H_Q + H_N \\ &= H_0 + H_{zee} + H_{hfs} \quad , \end{aligned}$$

where  $H_{zee} = \beta H (L + 2S) = \beta (g_x H_x S_x + g_y H_y S_y + g_z H_z S_z)$

is the Zeeman energy term,

$$H_{hfs} = A_x S_x I_x + A_y S_y I_y + A_z S_z I_z$$

is the hyperfine structure term,

$H_0$  contains several complex terms which are not important for EPR analysis of radiation damage centres, including electronic, crystal field, spin-orbit coupling, spin-spin coupling, quadrupole moment, and nuclear spin terms,

$S$  is the spin angular momentum operator,

$L$  is the orbital angular momentum operator,

$H$  is the applied magnetic field,

$g$  is the g-factor tensor,

$A$  is the hyperfine coupling tensor,

$\beta$  is the Bohr Magnetron,

and all z-components are considered to be directed parallel to the applied

magnetic field.

By EPR, the components of the g-tensor and of the A-tensor may be measured. From this, the orientation of the principal axes of these tensors may be determined, whereupon much information can be derived concerning the neighbourhood of the centre. Additional information may be obtained by studying the intensities of the resonant absorptions, and the dependence of these intensities on time and temperature.

#### C. Low Temperature Radiation Damage in Crystals

Incident high energy photons, such as x-rays, undergo a series of collisions inside of a sample. One of the possible mechanisms which accounts for the energy loss by these photons is the production of radiation defects, such as the ionization of impurity ion valence electrons or the formation of colour centres. When the irradiation process is terminated, the radiation damage products exhibit a decay with time, either back to the preradiation state, or to some other intermediate state. Such decay is referred to as annealing, and is often enhanced by heating or by bleaching the sample. As a result, low temperatures are often required in radiation damage experiments in order to arrest the rate of annealing. Otherwise, some of the EPR species might disappear before it is even possible to observe them in the spectrometer.

## II. INSTRUMENTATION

### A. X-Band Bridge Spectrometer

A block diagram of the x-band balanced bridge type of spectrometer, which was employed in these experiments, and which has been discussed in detail elsewhere<sup>7</sup>, is presented in Figure 1.

### B. Cryostat for Low Temperature Radiation Damage Studies

In order to study the EPR spectra of crystals irradiated at temperatures near the boiling point temperatures of liquid nitrogen or of liquid helium, a specially designed cryostat is required. A cross-section of the cryostat used in these experiments is presented in Figure 2. The cryostat is divided into two main sections: (1) a large main body to provide reservoirs (K,L) for the cryogenic liquids, and (2) a detachable tail consisting of a reservoir extension (Q), a copper radiation shield (R), and a stainless steel outer jacket (S). A vacuum tight seal (M) semi-permanently attaches the reservoir extension to the centre reservoir (K). The radiation shield is mounted to a flange (N) that is in thermal contact with the liquid nitrogen reservoir (L). A rubber O-ring forms a vacuum tight seal (O) between the tail jacket and the flange which terminates the outer wall of the cryostat. Through this flange pass six vacuum tight feed-throughs (P) for electrical leads. The cryostat is evacuated by means of a high vacuum service valve (F). This vacuum insulates the centre reservoir from the liquid nitrogen reservoir and its accompanying tail radiation shield,

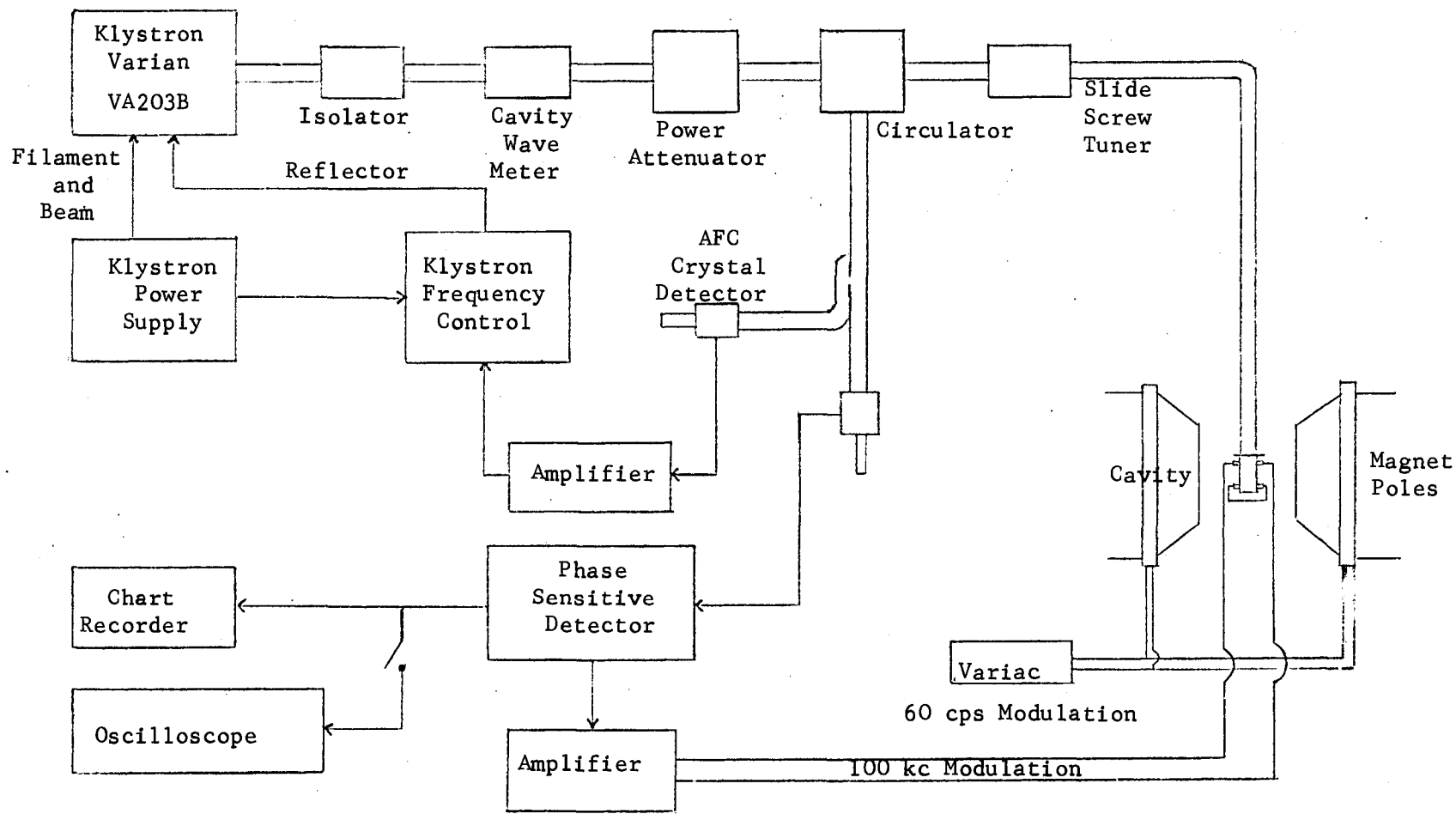


Fig. 1. Block diagram of x-band spectrometer used for EPR experiments at temperatures near 77°K.

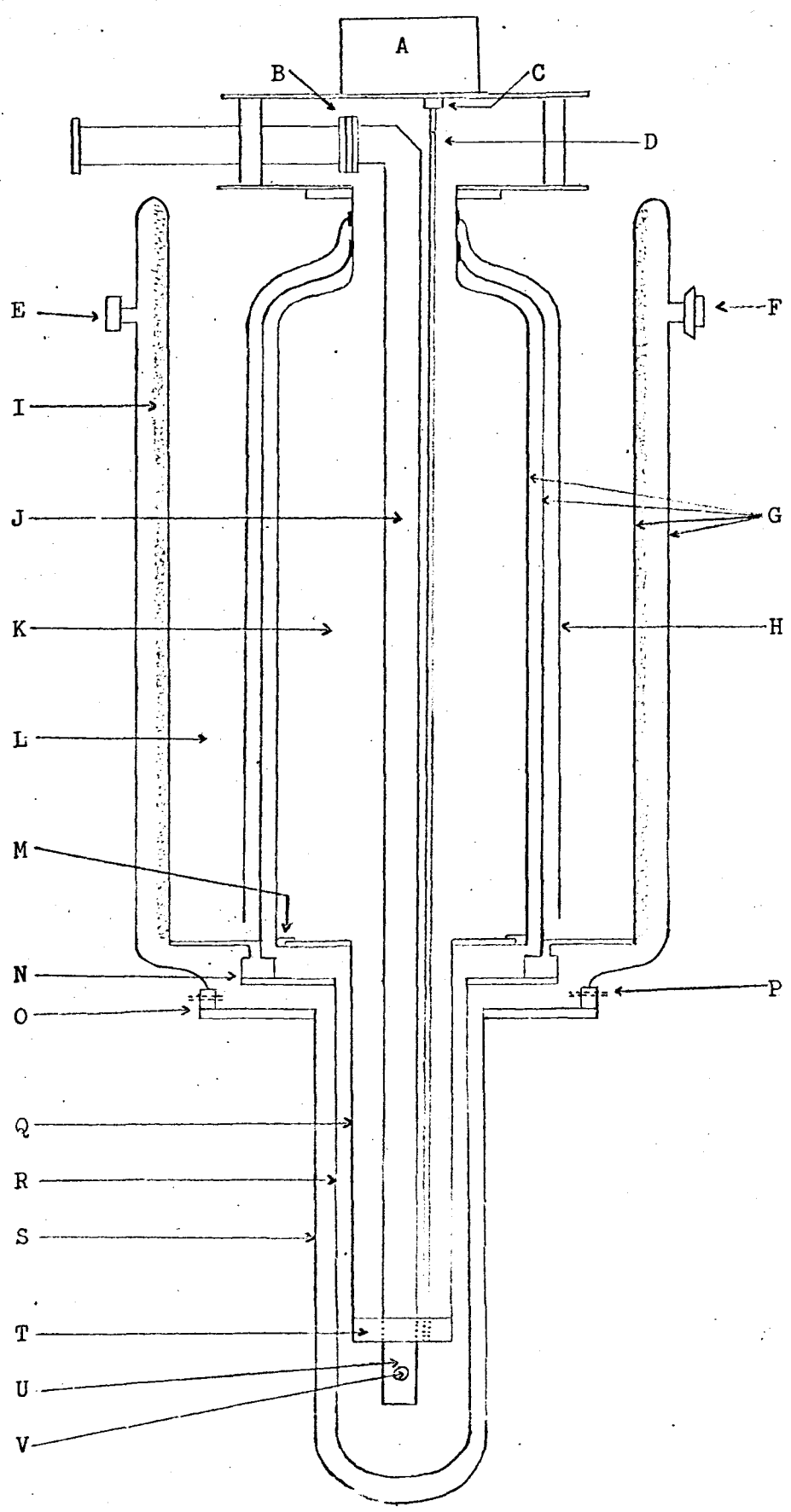


Fig. 2. Cross section of EPR Cryostat used to study low temperature radiation damage in crystals.

and, in turn, these from the atmosphere. The thermal insulation of the liquid nitrogen reservoir is further enhanced by the presence of milar (I) in the vacuum between the outermost walls. With the exception of copper shield (H), which encloses the centre reservoir within a surrounding near the boiling point temperature of liquid nitrogen irregardless of the liquid nitrogen level, all the cryostat walls (G) in the main body are constructed from stainless steel. Above the cavity (V), a waveguide (J) and a tube (D) for a crystal rotator shaft, both made from stainless steel and evacuated, pass through the brass block (T) that terminates the reservoir extension and extend up through the centre reservoir to the top of the cryostat. Here, a mica window (B) sealed with indium ends the waveguide vacuum while a special double O-ring seal (C), illustrated in Figure 3, closes off the tube, but yet allows the rotator shaft to turn. Above this seal sits a housing (A) for the crystal rotator and crystal orientation indicator. A final feature illustrated in Figure 2 is a safety release valve (E) that ruptures at high pressures.

The cut-away view of the tail assembly presented in Figure 4 shows in greater detail some features of the cryostat. The crystal rotator shaft (A), worm (C), and gear (G) assembly was discussed in detail elsewhere<sup>7,8</sup>. The sample (E) sits on a nylon pin (F) inserted into the gear. A small hole bored up the centre of the pin provides access to the sample for temperature monitoring by thermocouple (H) without harming the cavity Q. A second thermocouple (M) determines the temperature of the cavity which is coupled to the waveguide (B) by means of an iris (D). In order to overcome the severe attenuation of 100 k.c. field

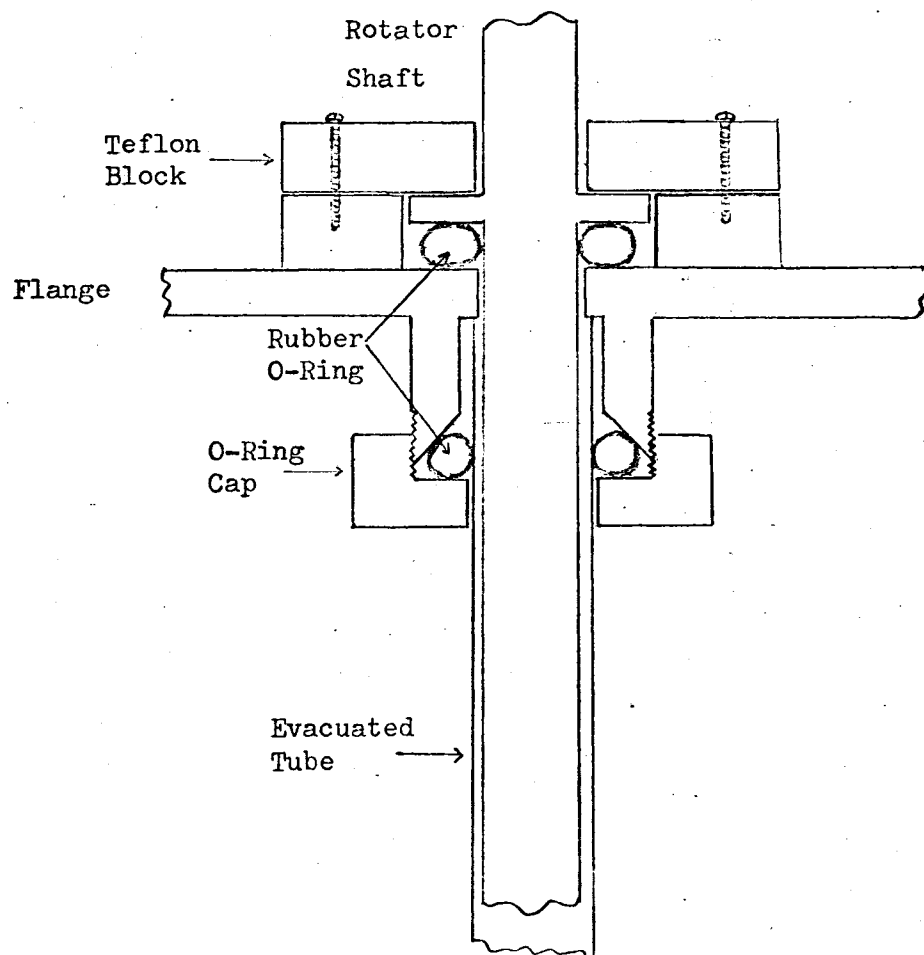


Fig. 3. Vacuum seal for crystal rotator.



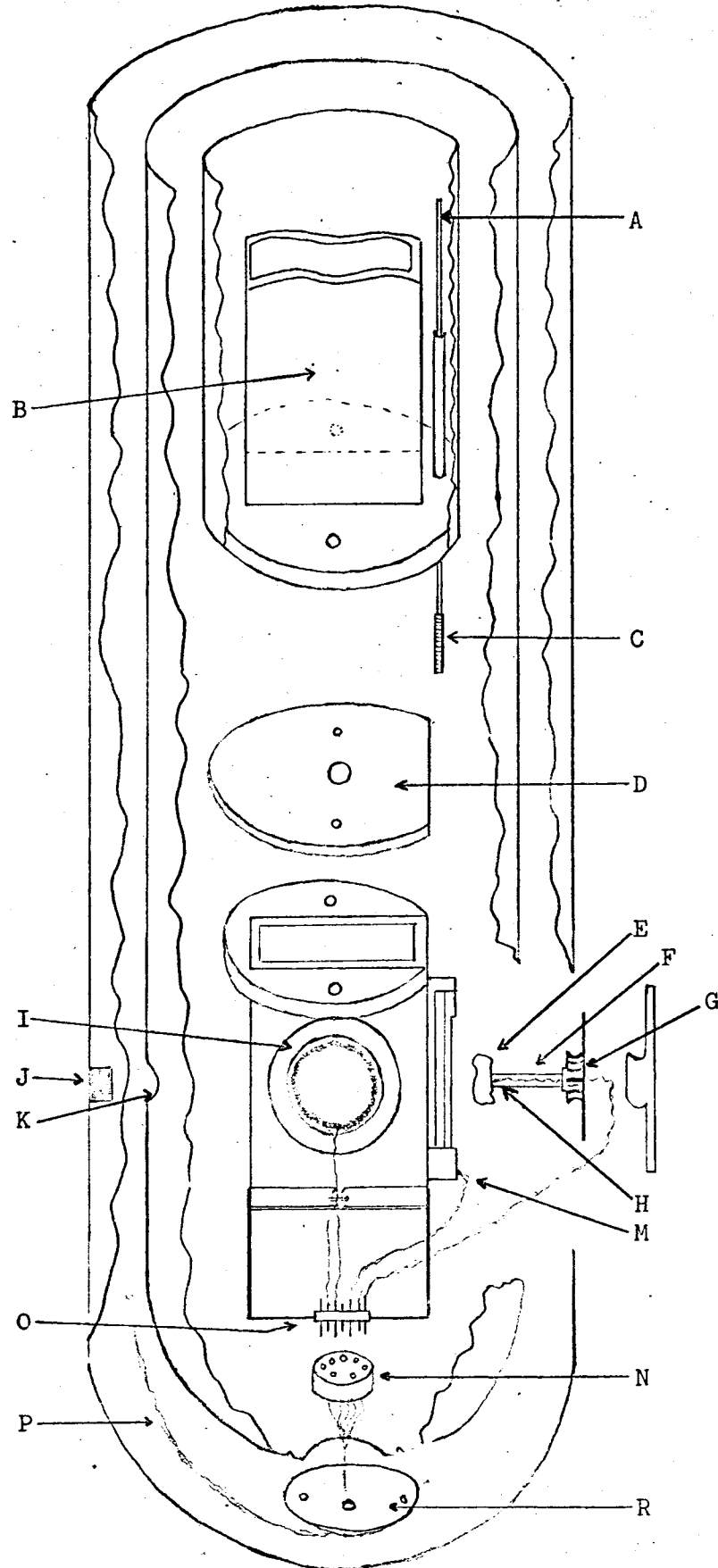


Fig. 4. Cut-away view of the cryostat tail assembly.

modulation by the cavity walls, special plugs (I) of brass foil of a thickness intermediate between the skin depths of the microwave power and of the 100 k.c. radiation are fitted tightly into holes centred on the broad sides of the cavity. Good electrical contact and smooth continuous surfaces on the inside walls of the cavity are required in order to maintain a large cavity Q. Small coils (L) were inserted into the plugs to provide the 100 k.c. field modulation. The modulation coil leads and the thermocouple leads terminate at a small plug (O) strapped to the cavity as shown. Teflon-coated wires (P) connect the electrical feed-throughs (Figure 2) with a socket (N) mated with this plug. The socket is easily separated from the plug and withdrawn through a hole in the radiation shield to facilitate cryostat dismantling. Most of this radiation shield hole is covered over by a copper cap (R) when the cryostat is assembled. Figure 4 also shows the special beryllium window (J) in the tail jacket and the radiation shield hole (K) which provide access to the sample for the x-radiation.

A cross section of the rectangular  $TE_{102}$  resonant cavity presented in Figure 5 illustrates further how the cavity was modified in order to produce 100 k.c. field modulation at the sample site.

### C. Sample Alignment

When the cryostat is positioned vertically, as must be the case when it is filled with liquid nitrogen or liquid helium, the beryllium window, the radiation shield hole, the cavity hole, and the sample are aligned along a horizontal axis. However, the x-ray beam leaving the x-ray tube is inclined downward at about  $5^\circ$  from the

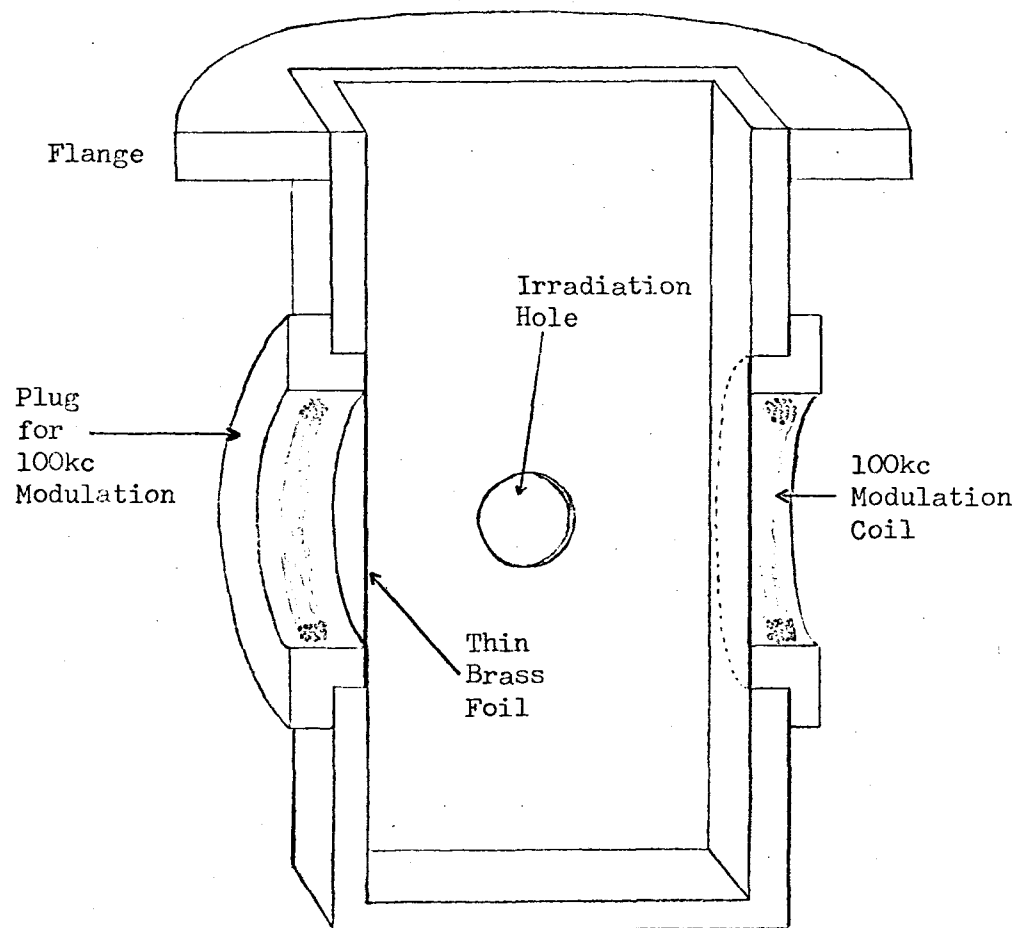


Fig. 5. Cross-section of resonant cavity adapted for 100 kc field Modulation.

horizontal. As a result, it was necessary to tilt the cryostat and to carefully position it in front of the x-ray source so that the highest possible intensity of the x-ray beam actually arrived at the sample position. The cryostat was assembled as shown in Figure 6(a), and film located in front of the cavity, in back of the cavity, and in the centre of the cavity was exposed. Following each exposure, the cryostat was carefully repositioned until a set of photographs were obtained, the prints of which are presented in Figure 6(b).

#### D. Sample and Cavity Temperatures

Copper-constantan thermocouples were employed to monitor the temperature of the sample and of the cavity during experiments. It was found that during the x-irradiation process, the sample temperature was about  $100^{\circ}\text{K}$ , while that of the cavity was about  $87^{\circ}\text{K}$ . These, however, were not the temperatures observed during operation of the EPR spectrometer. Passage of a current through the 100 k.c. modulation coils located on the cavity sides generated a quantity of heat which effectively raised these temperatures to about  $105^{\circ}\text{K}$  for both sample and the cavity.

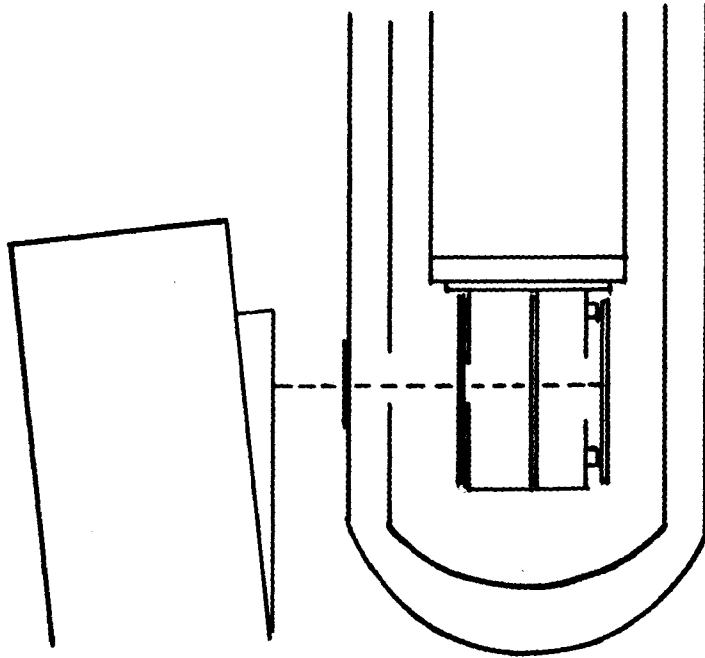


Fig. 6(a). Method of sample alignment for x-irradiation.

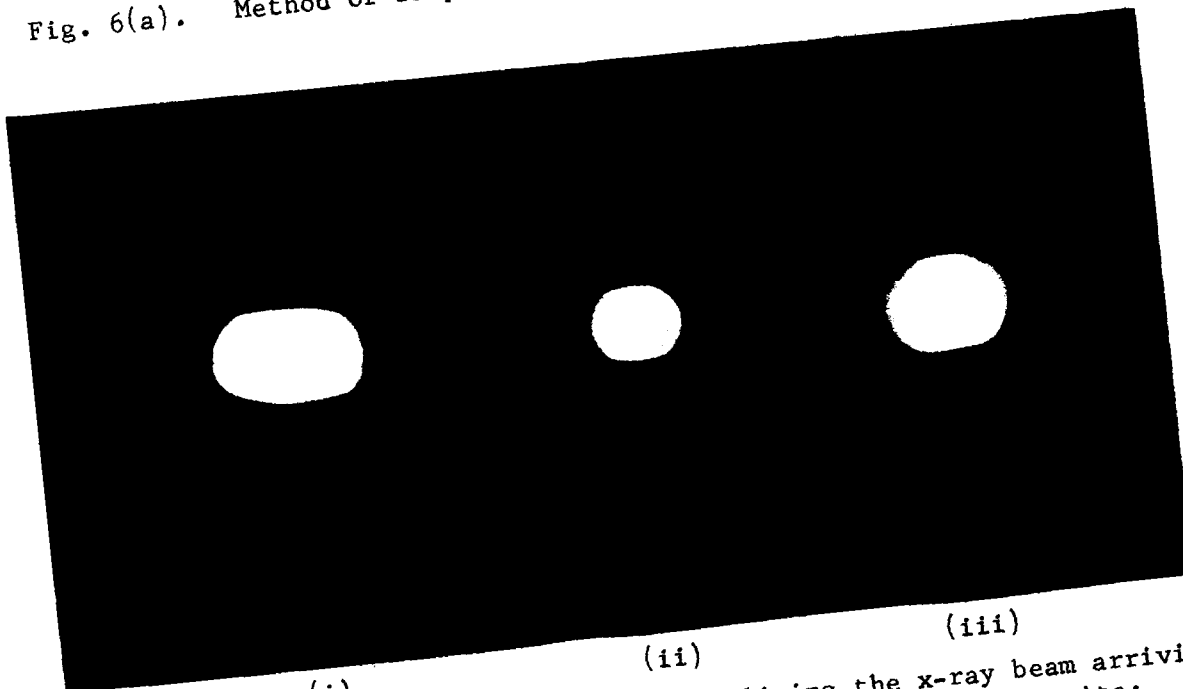


Fig. 6(b). Print of film exposures outlining the x-ray beam arriving  
 (i) in front of the cavity; (ii) at the sample site;  
 (iii) at the back wall of the cavity.

### III. EXPERIMENTAL PROCEDURE

The EPR spectra of the samples were recorded at low temperature before and after irradiation with hard x-rays (40 - 50 Kev). The recorded spectra were then compared for possible spectrum changes resulting from radiation damage. Where appreciable changes had occurred, the spectrum was recorded once more after it had warmed up to room temperature to note if such changes continued to persist.

In the course of these experiments, the samples were each irradiated for about 2 hours. They were subjected to a rate of radiation dosage corresponding to an 18 milliamperere x-ray tube current. The x-rays leaving the source passed through about 2 cm. of air, a thin beryllium window in the cryostat tail, and a few centimetres of vacuum before reaching the sample. Hence, the actual amount of radiation arriving at the sample was only slightly attenuated.

#### IV. RESULTS AND DISCUSSION

##### A. Natural Phenacite

Changes occurred in the spectrum of Phenacite following x-irradiation of the sample at  $100^{\circ}\text{K}$ . These changes are illustrated in Figure 7. A comparison of Figure 7(a) with Figure 7(b) indicates the appearance of two additional groups of absorption lines located almost equally distant on either side of the original spectrum. These groups appeared to be triplets, and continued to exist even after the sample had been warmed to room temperature. Figure 8 shows in greater detail the changes in the central group. There was an increase in the number of resonance lines in this group after low temperature irradiation. However, when the sample was warmed to  $292^{\circ}\text{K}$ , the spectrum appeared to have changed again. This would seem to indicate an annealing of some radiation damage centres in Phenacite within the temperature range of  $100^{\circ}\text{K}$  to  $292^{\circ}\text{K}$ .

##### B. Calcium Fluoride Containing Iron Impurities

The EPR spectrum of the  $\text{CaF}_2:\text{Fe}$  sample showed marked change following low temperature x-irradiation. The spectrum coming from the unirradiated crystal at  $100^{\circ}\text{K}$  appeared as a single group of resonance lines centred about the DPPH resonance [Figure 9(a)]. After irradiation, the spectrum had changed to five sets of resonance lines centred approximately about DPPH [Figure 9(b)]. When the sample was warmed to  $292^{\circ}\text{K}$  [Figure 9(c)], the spectrum resembled that obtained from the unirradiated

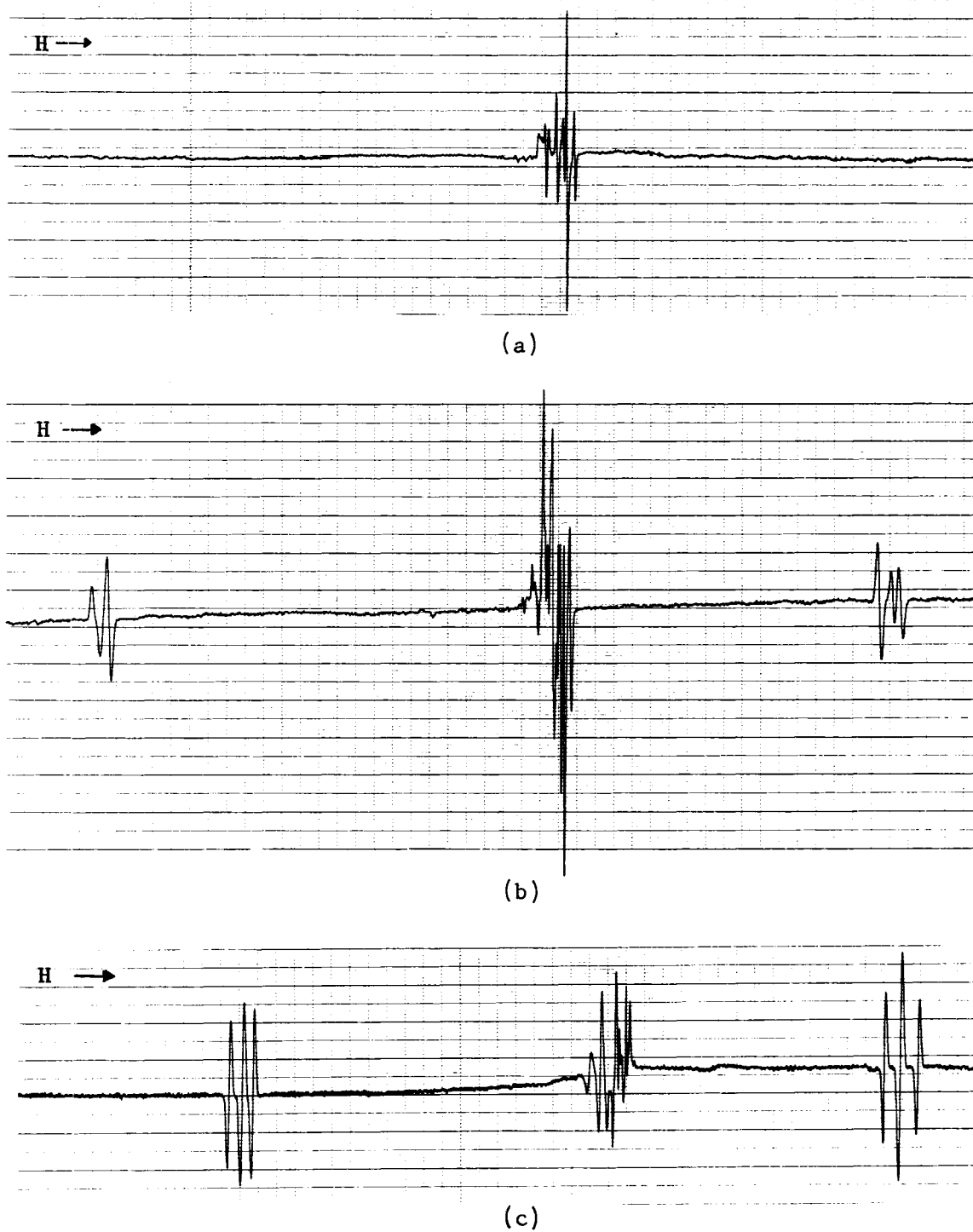
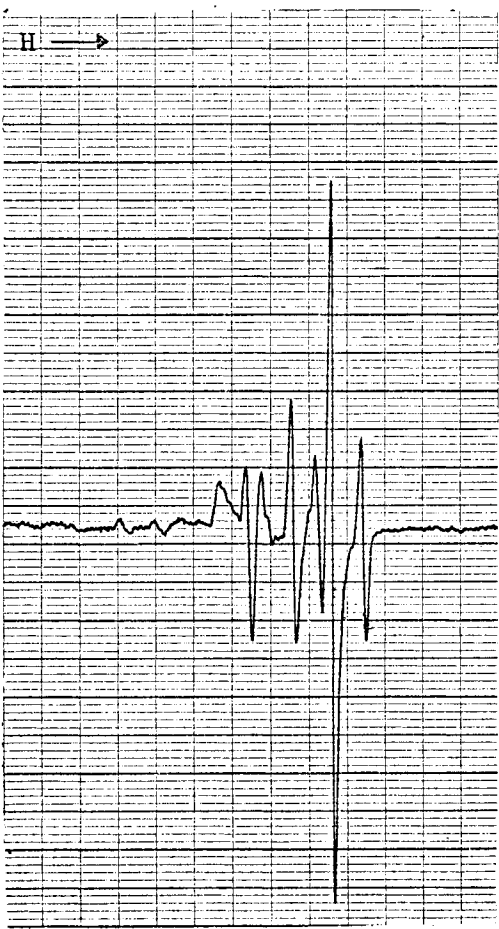
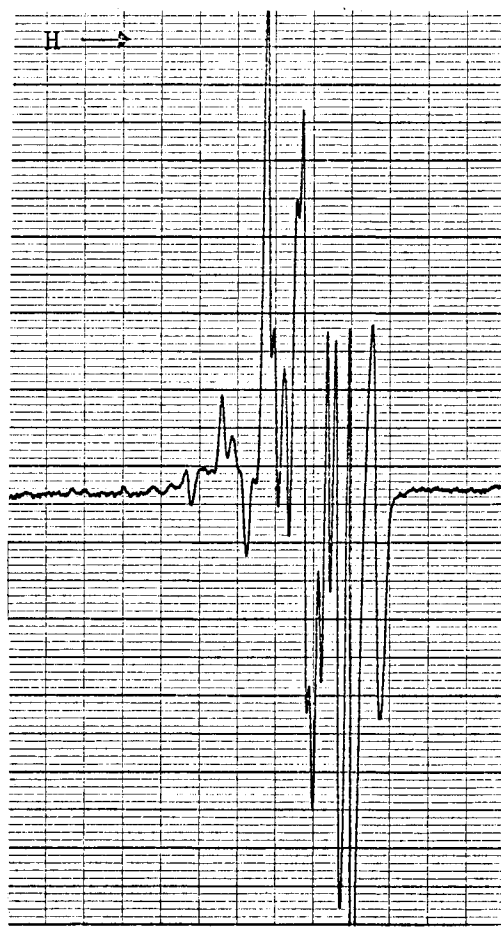


Fig. 7. Comparison of Phenacite spectrum (a) at  $100^{\circ}\text{K}$  before x-irradiation, (b) at  $100^{\circ}\text{K}$  after x-irradiation, and (c) at room temperature following x-irradiation at  $100^{\circ}\text{K}$ . Sample orientation in part (c) is not the same as in parts (a) and (b).

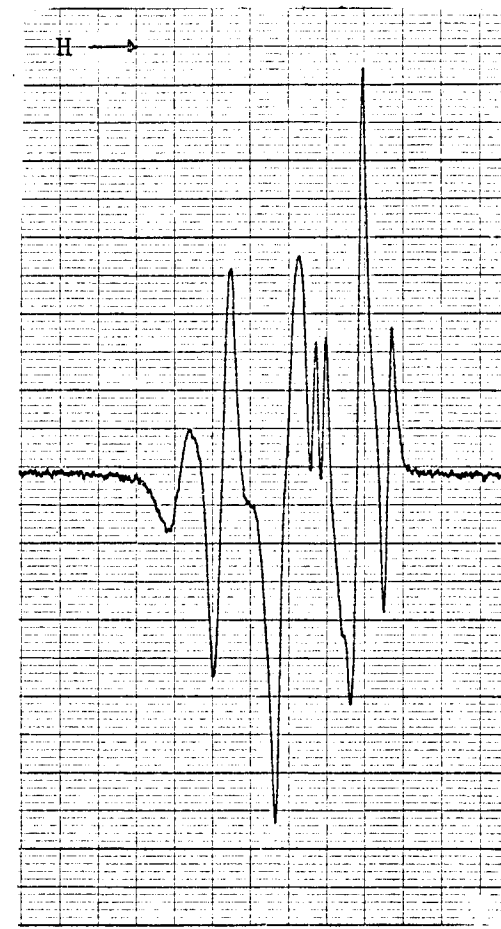




(a)



(b)



(c)

Fig. 8. A detailed comparison of the central group of spectrum in Phenacite (a) at 100°K before x-irradiation, (b) at 100°K after x-irradiation, (c) at room temperature following x-irradiation at 100°K. Sample orientation in part (c) differs from that of parts (a) and (b).

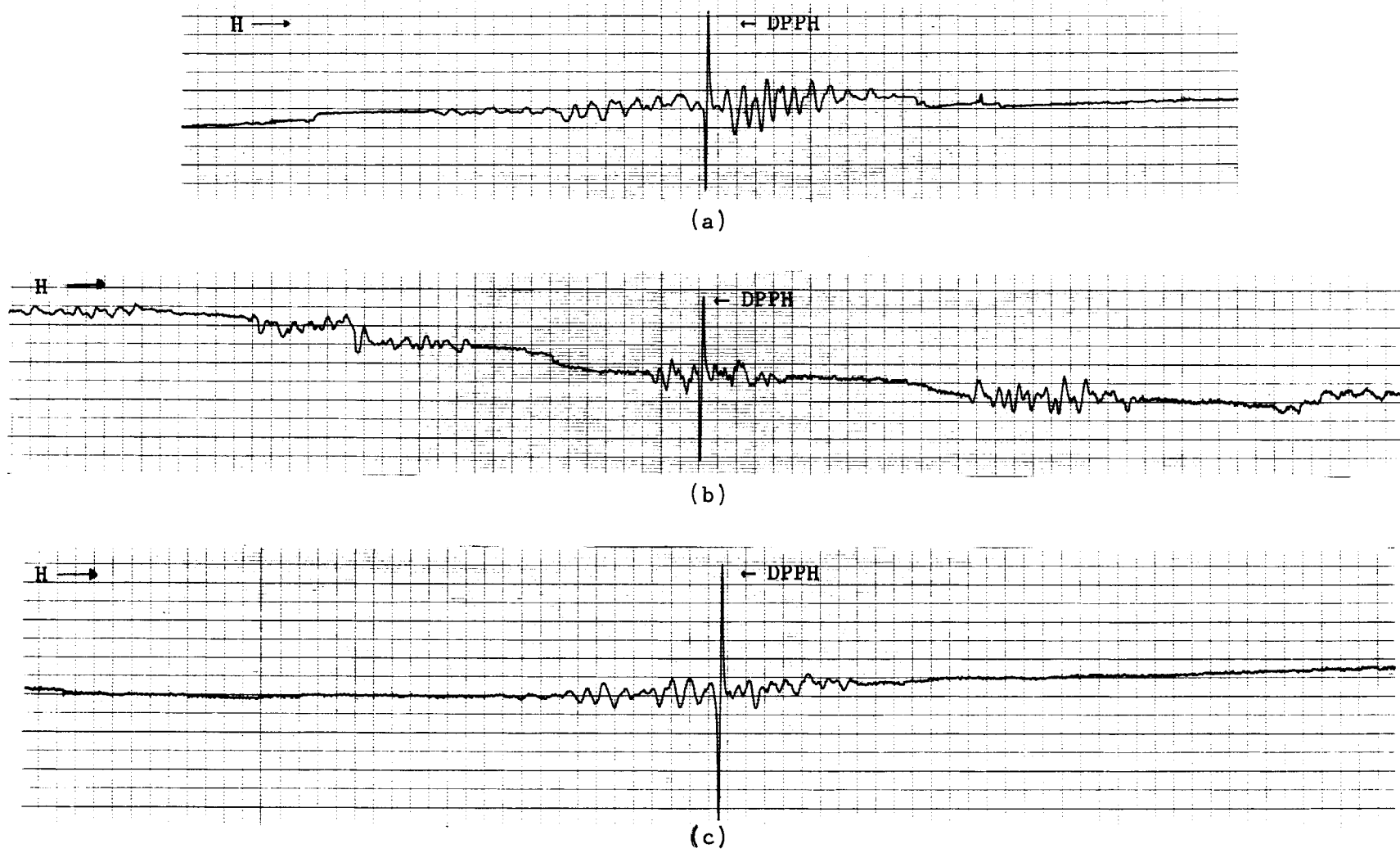


Fig. 9. Comparison of  $\text{CaF}_2:\text{Fe}$  spectrum (a) at  $100^\circ\text{K}$  before x-irradiation, (b) at  $100^\circ\text{K}$  after x-irradiation, and (c) at room temperature following x-irradiation at  $100^\circ\text{K}$ .

sample.

The changes in the EPR spectrum of the  $\text{CaF}_2:\text{Fe}$  sample were also studied during the period when it was allowed to warm up following x-irradiation at  $100^\circ\text{K}$ . These studies were carried out with the magnetic field oriented differently than it was in the first case discussed above. The observed changes in the spectrum are presented in Figures 10 and 11. The spectrum obtained before irradiation at  $100^\circ\text{K}$  is shown in Figure 10(a). That obtained immediately after the crystal was x-irradiated at  $100^\circ\text{K}$  is presented in Figure 10(b). The recording traces in Figure 11 were obtained while the crystal was then allowed to warm up to room temperature. It is seen that the EPR spectrum changes from a single group of resonance lines [Figure 10(b)] to three groups [Figure 10(a)], and then back again to one group [Figures 11(b), 11(c)], as the temperature of the crystal increases to  $292^\circ\text{K}$ . Moreover, Figure 11(c) exhibits a spectrum somewhat similar to that obtained from the unirradiated  $\text{CaF}_2:\text{Fe}$  sample at  $100^\circ\text{K}$  [Figure 10(a)]. Hence, it seems probable that most of the paramagnetic radiation damage centres in the  $\text{CaF}_2:\text{Fe}$  sample produced by x-irradiation at  $100^\circ\text{K}$  are annealed by warming the sample to room temperature.

#### C. Barium Fluoride Containing Chromium Impurities

No changes were observed in the EPR spectrum of  $\text{BaF}_2:\text{Cr}$  following irradiation of the crystal at  $100^\circ\text{K}$  with 48 keV x-rays. The recording trace in Figure 12(a) shows only the DPPH resonance line in the EPR spectrum of the sample at  $100^\circ\text{K}$  before irradiation. Similarly, the spectrum of the sample after irradiation at  $100^\circ\text{K}$  [Figure 12(b)] contains only the DPPH resonance line. Hence if any EPR radiation

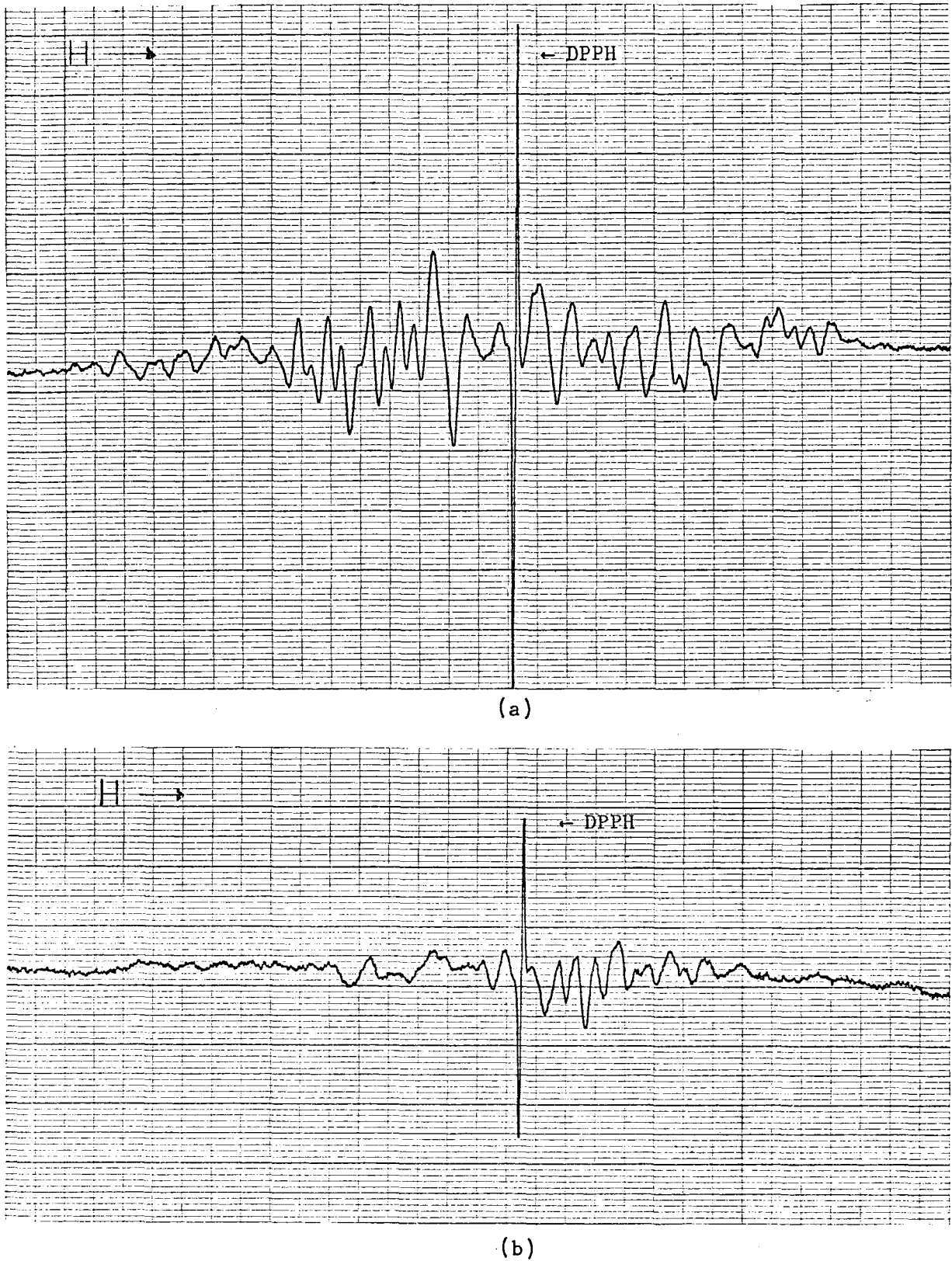


Fig. 10. Comparison of  $\text{CaF}_2:\text{Fe}$  spectrum at a second orientation (a) at  $100^\circ\text{K}$  before irradiation and (b) at  $100^\circ\text{K}$  after irradiation.

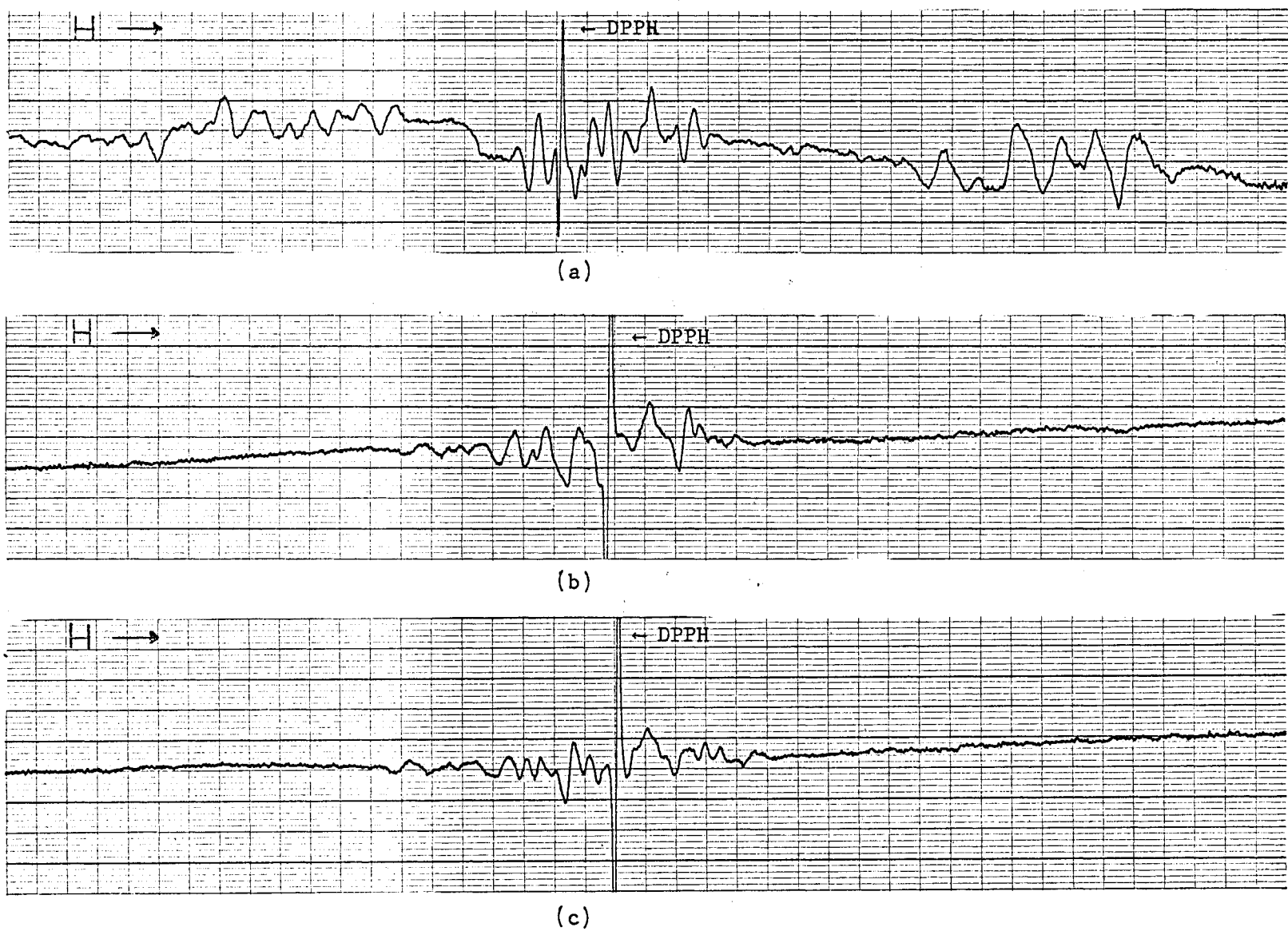


Fig. 11. Changes in the  $\text{CaF}_2:\text{Fe}$  spectrum at the sample orientation of Figure 10 during warming period following x-irradiation at  $100^\circ\text{K}$ . Part (a) shows the spectrum at some intermediate temperature, (b) the spectrum at almost room temperature, and (c) the spectrum at room temperature. Time interval between recordings was about 1/2 hour.

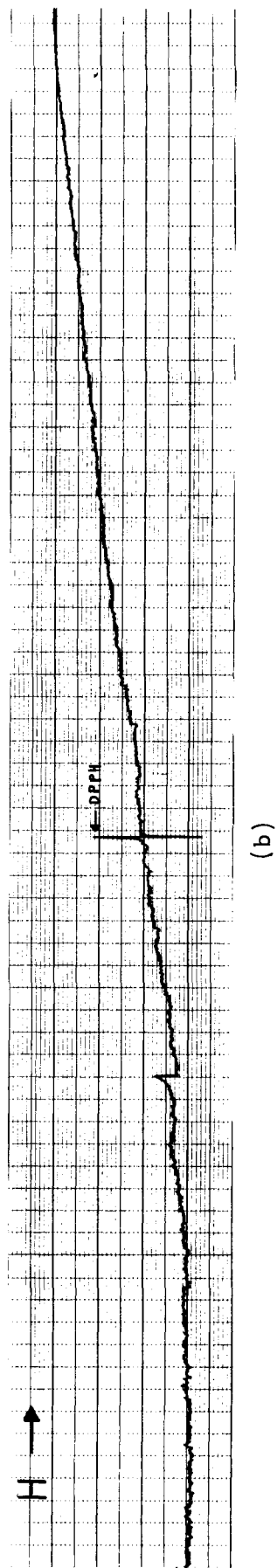
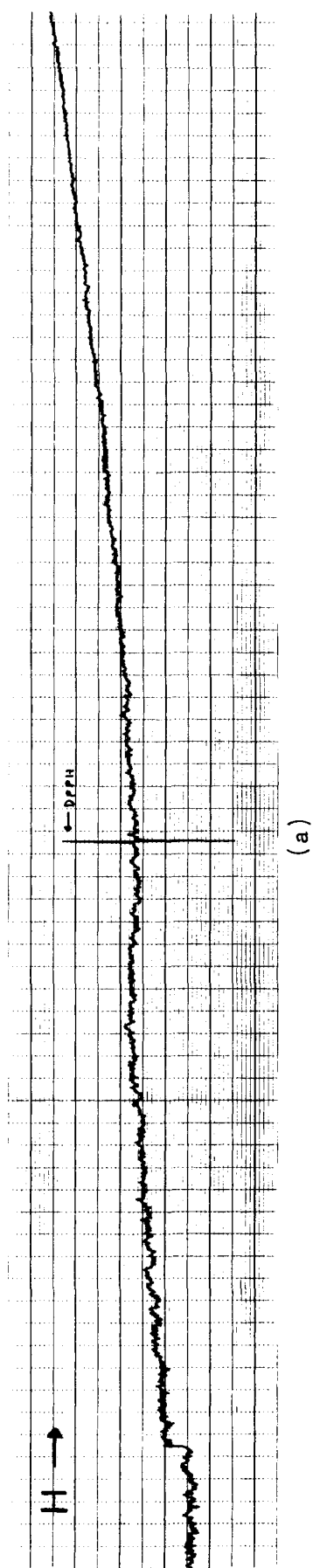


Fig. 12. EPR spectrum of  $\text{BaF}_2:\text{Cr}$  (a) at  $100^\circ\text{K}$  before x-irradiation, and (b) at  $100^\circ\text{K}$  after irradiation.

damage centres were produced during the x-irradiation at  $100^{\circ}\text{K}$ , they were annealed immediately and completely.

#### REFERENCES

1. E. Goldstein, *Zeits f. Instrumentenkunde*, 16, 211 (1896).
2. R. W. Pohl, *Proc. Phys. Soc.* 49, 3 (1937).
3. F. Seitz, *Rev. Mod. Phys.* 26, 7 (1954).
4. H. Pick, *Nuovo Cimento Suppl.* 7, 498 (1958).
5. Seidel and Wolf, *Phys. Status Solidi* 11, 3 (1965).
6. Clyde A. Hutchinson, Jr., *Phys. Rev.* 75, 1769 (1949).
7. S. M. Quick, M.Sc. Thesis, Department of Physics, University of Windsor, Windsor, Ontario, (1966).
8. Armen Manoogian, M.Sc. Thesis, Department of Physics, University of Windsor, Windsor, Ontario, (1966).
9. Charles P. Poole, *Electron Spin Resonance*, (Interscience Publishers, New York) 1967.



VITA AUCTORIS

The author was born in Windsor, Ontario, on March 24, 1942 and received his early education there. In 1962, he enrolled in the Honours Physics and Mathematics course at the University of Windsor, and graduated there with a B.Sc. degree in Physics in 1966.

177171

25

**UNIVERSITY OF WINDSOR LIBRARY**